⌘ *Author's Choice*

THE JOURNAL OF BIOLOGICAL CHEMISTRY VOL. 285, NO. 51, pp. 40397–40408, December 17, 2010

Vibrio cholerae ParE2 Poisons DNA Gyrase via a Mechanism Distinct from Other Gyrase Inhibitors*[S]

Received for publication, April 27, 2010, and in revised form, September 23, 2010 Published, JBC Papers in Press, October 15, 2010, DOI 10.1074/jbc.M110.138776

Jie Yuan[‡§¶], **Yann Sterckx**[‖**1], **Lesley A. Mitchenall**[‡‡], **Anthony Maxwell**[‡‡], **Remy Loris**[‖**], **and Matthew K. Waldor**[‡§¶2]

From the [‡]*Channing Laboratory, Brigham and Women's Hospital, Harvard Medical School, the* [§]*Howard Hughes Medical Institute, and the* [¶]*Program in Immunology, Tufts University School of Medicine, Boston, Massachusetts 02115,* [‖]*Structural Biology Brussels, Vrije Universiteit Brussel Pleinlaan 2, Brussels 1050, Belgium, the* **Department of Molecular and Cellular Interactions, Vlaams Instituut voor Biotechnologie, Pleinlaan 2, Brussels 1050, Belgium, and the* [‡‡]*Department of Biological Chemistry, John Innes Centre, Colney, Norwich NR4 7UH, United Kingdom*

DNA gyrase is an essential bacterial enzyme required for the maintenance of chromosomal DNA topology. This enzyme is the target of several protein toxins encoded in toxin-antitoxin (TA) loci as well as of man-made antibiotics such as quinolones. The genome of *Vibrio cholerae*, the cause of cholera, contains three putative TA loci that exhibit modest similarity to the RK2 plasmid-borne *parDE* TA locus, which is thought to target gyrase although its mechanism of action is uncharacterized. Here we investigated the *V. cholerae parDE2* locus. We found that this locus encodes a functional proteic TA pair that is active in *Escherichia coli* as well as *V. cholerae.* ParD2 co-purified with ParE2 and interacted with it directly. Unlike many other antitoxins, ParD2 could prevent but not reverse ParE2 toxicity. ParE2, like the unrelated F-encoded toxin CcdB and quinolones, targeted the GyrA subunit and stalled the DNA-gyrase cleavage complex. However, in contrast to other gyrase poisons, ParE2 toxicity required ATP, and it interfered with gyrase-dependent DNA supercoiling but not DNA relaxation. ParE2 did not bind GyrA fragments bound by CcdB and quinolones, and a set of strains resistant to a variety of known gyrase inhibitors all exhibited sensitivity to ParE2. Together, our findings suggest that ParE2 and presumably its many plasmid- and chromosome-encoded homologues inhibit gyrase in a different manner than previously described agents.

Toxin-antitoxin (TA)[3] loci encode a toxic protein (the toxin) and an antitoxin, either RNA or protein, that can neutralize the toxin activity. TA loci were originally identified in low copy plasmids (1, 2), where they ensure plasmid maintenance by killing plasmid-free daughter cells in a process known as post-segregational killing (3). Plasmid-borne TA loci promote plasmid maintenance because antitoxins are more labile than their cognate toxins in the intracellular environment. Plasmid-free cells, which can no longer synthesize either toxin or antitoxin, are therefore subject to the growth inhibitory/killing effect of the relatively long-lived toxin. Although TA loci were initially discovered in plasmids, in the current "post-genomic era," it has become clear that these loci are also present in the chromosomes of nearly all species of bacteria, often in multiple copies (4). Some bacteria harbor very large numbers of TA loci in their chromosome (5), typically in association with mobile genetic elements. For example, in *Vibrio cholerae*, 13 TA loci are found associated with *attC* recombination sequences,which apparently enabled their capture by the integrase of the chromosome 2 superintegron (6). Even though the biochemical activities of several chromosome-encoded toxins have been deciphered, the physiologic significance of these ubiquitous loci remains the subject of controversy (7–9).

CcdB and ParE are representative of two families of unrelated toxins that block DNA replication by inhibiting DNA gyrase, an essential enzyme that is also the target of quinolone antibacterial agents (10). ParE, a toxin encoded on plasmid RK2 (11–13), and CcdB, a toxin encoded on the F plasmid, have unrelated amino acid sequences, but they both poison DNA gyrase. CcdB and ParE are encoded adjacent to proteic antitoxins, known as CcdA and ParD, respectively. Proteins similar to CcdB and ParE are encoded within plasmid and chromosomal sequences (4). Chromosomal CcdB homologues have been shown to target gyrase (14), but studies demonstrating that chromosomal ParE homologues poison this essential enzyme have not been reported.

Like other type II topoisomerases, DNA gyrase modifies DNA topology by introducing a double-stranded break in DNA through which a second DNA duplex is passed (15). This process can result in relaxation of positive or negative supercoils, both of which are energetically favored. Gyrase can also introduce negative supercoils; this process requires ATP. Both transcription and DNA replication generate positively supercoiled DNA, and gyrase is required to relieve the topological stresses associated with these essential processes. Maintenance of correct levels of chromosomal superhelicity is

* This work was supported, in whole or in part, by National Institutes of Health Grant R37 AI-42347. This work was also supported by the Howard Hughes Medical Institute (to M. K. W.). Part of this work was supported by grants from Vlaams Instituut voor Biotechnologie, Vrije Universiteit Brussel and FWO-Vlaanderen. This work was also supported by the Biotechnology and Biological Sciences Research Council, Swindon, United Kingdom (to A. M.).

⌘ *Author's Choice*—Final version full access.

[S] The on-line version of this article (available at http://www.jbc.org) contains supplemental Figs. 1–6.

[1] Recipient of an individual predoctoral fellowship from FWO-Vlaanderen.

[2] To whom correspondence should be addressed: 181 Longwood Ave., Brigham and Women's Hospital, Boston, MA 02115. Fax: 617-525-4660; E-mail: mwaldor@rics.bwh.harvard.edu.

[3] The abbreviations used are: TA, toxin-antitoxin; CFU, colony-forming units; IPTG, isopropyl-β-D-thiogalactopyranoside; Ni-NTA, nickel-nitrilotriacetic acid; SPR, surface plasmon resonance; ATPγS, adenosine 5′-*O*-(thiotriphosphate); Nal, nalidixic acid.

also critical for initiation of DNA replication and for the formation of open complexes for initiation of transcription (16).

Gyrase is a tetramer composed of two GyrA and two GyrB subunits, and both subunits contain distinct functional domains. The N-terminal domain of GyrA catalyzes the cleavage and rejoining of DNA, and its C-terminal domain binds and wraps DNA around the enzyme. Without the GyrA C-terminal domain (GyrA-CTD), also called the "DNA wrapping domain" or GyrA33 (17), gyrase is unable to negatively supercoil DNA; however, it still retains low levels of relaxation activity (18). The N-terminal domain of GyrB binds and hydrolyzes ATP, whereas its C-terminal domain interacts with GyrA and DNA (16, 19).

The mechanism of action of relatively few gyrase inhibitors has been determined. CcdB has been found to bind the dimerization domain of GyrA, thereby preventing strand passage as well as closure of the enzyme. In the presence of CcdB, the covalently linked DNA gyrase reaction intermediates are stabilized, which generates a "road block" for cellular polymerases *in vivo* and detectable DNA fragmentation *in vitro* (20). Quinolone antibiotics, such as nalidixic acid, also stabilize DNA gyrase intermediates, although they and CcdB target distinct sites within GyrA (16). ParE from plasmid RK2 is also thought to poison gyrase by stabilizing gyrase-DNA complexes, but the interactions between ParE and gyrase subunits and the mechanism by which ParE inhibits gyrase have not been explored. An *Escherichia coli* strain harboring a CcdB-resistant GyrA was not resistant to RK2-encoded ParE, raising the possibility that ParE inhibits gyrase in a different manner than CcdB (11). Putative ParDE homologues are encoded in the genomes of a wide variety of Gram-negative and Gram-positive bacteria (4, 21), but studies of the target and mechanisms of these chromosome-borne TA systems have not been conducted.

Here, we investigated the activities encoded by the *parDE2* locus found in the *V. cholerae* superintegron. In this Gram-negative rod, the cause of cholera, the 13 putative TA loci include 3 loci with modest similarity to *parDE* of RK2. The predicted ParE2 amino acid sequence exhibits 29% sequence identity with RK2-ParE, whereas the predicted ParD2 sequence is only 12% identical to RK2 ParD. We found that the *V. cholerae parDE2* genes encode a functional TA pair. Overexpression of ParE2 inhibited the growth of both *V. cholerae* and *E. coli*. ParD2 could prevent but not reverse ParE2 toxicity and, thus, may function in a different fashion than many other antitoxins. ParD2 co-purified along with ParE2, suggesting that ParD2-mediated neutralization of ParE2 toxicity results from the *in vivo* formation of a ParE2-ParD2 protein complex. Gyrase also co-purified with ParE2; *in vitro* studies revealed that distinct sites within GyrA are bound by ParE2 and CcdB. Unlike quinolones and CcdB, ParE2 requires ATP to stabilize gyrase-DNA cleavage complexes. In aggregate, our findings suggest that ParE2 inhibits gyrase in a different manner from other gyrase toxins.

EXPERIMENTAL PROCEDURES

Bacterial Strains and Plasmids—The plasmids and strains used in this study are listed in Table 1. All the gyrase mutant strains were generously provided by Coli Genetic Stock Center at Yale University. Bacteria were grown in LB medium at 37 °C. Antibiotics were used at the following concentrations: streptomycin, 200 μg/ml; kanamycin, 50 μg/ml; chloramphenicol, 20 μg/ml for *E. coli* and 5 μg/ml for *V. cholerae*.

TABLE 1
Strains and plasmids used in this study

Name	Relevant description	Source or reference
Strains		
N16961	*V. cholerae* El Tor biotype	Ref. 26
JY367	N16961/pBAD33*parE2*+pGZ*parD2*	This study
JY370	N16961/pBAD33*parE2*+pGZvector	This study
BW27784		Ref. 28
JY 233	BW27784/pBAD33*parE2*+pGZ*parD2*	This study
JY569	BW27784/pBAD33*parE2*+pGZvector	This study
BL21(DE3)		Novagen
JY262	BL21(DE3)/pET28bHis*parD2*	This study
JY302	BL21(DE3)/pET28bHis*parE2*+pBAD33*parD2*	This study
JY307	BL21(DE3)/pET28bHis*parD2*+pBAD33*parE2myc*	This study
JY384	BL21(DE3)/pET28bHis*gyrA*	This study
JY444	BL21(DE3)/pET28bHis*gyrB*	This study
JY664	BL21(DE3)/pET28bHis*parD2*+pBAD33*ccdBv.f.*	This study
JY668	BL21(DE3)/pET28bHis*gyrA14*+pBAD33*ccdBv.f.*	This study
JY670	BL21(DE3)/pET28bHis*gyrA14*+pBAD33*parE2*	This study
JY281	DH5α/pBAD33*parE2myc*	This study
Plasmids		
pBAD33		Ref. 53
BAD33*parE2*	*parE2* gene in SacI-XbaI sites of pBAD33	This study
pBAD33*ccdBv.f.*	*V. fischeri ccdB* gene in SacI-XbaI sites of pBAD33	This study
pGZ119EH		Ref. 54
pGZ*parD2*	*parD2* gene in EcoRI-XbaI sites of pGZ119	This study
pET28b		Ref. 22
pET28b*parE2*	*parE2* gene in NdeI-XhoI sites of pET28b	This study
pET28b*parD2*	*parD2* gene in NdeI-XhoI sites of pET28b	This study
pET28b*gyrA*	*E. coli gyrA* in NdeI-XhoI sites of pET28b	This study
pET28b*gyrB*	*E. coli gyrB* in NdeI-XhoI sites of pET28b	This study
pET28b*gyrA14*	*E. coli gyrA14* in NdeI-BamHI sites of pET28b	This study

Mapping the 5′ End of the parD2 Transcript Analysis—Total RNA was extracted from N16961 using TRIzol (Invitrogen), and after DNase I (Qiagen) treatment, 5′ rapid amplification of cDNA ends was performed according to manufacturer's protocol (Invitrogen). The reverse transcription reaction was performed with JPP78 (TCATCGAATGTTTTCACTAT) and then PCR-amplified with the Abridged Anchor Primer (Invitrogen) and JPP80 (TGAAGCTATCAAGGTCATAATCAGCGTCA).

In Vivo ParE2 and ParD2 Activity Assays—*V. cholerae* and *E. coli* strains were grown in LB with appropriate antibiotics and 0.2% glucose to an A_{600} of ~0.3–0.5, spun down, washed twice with LB and then resuspended in LB with antibiotics and either 0.2% glucose or 0.02% arabinose and grown at 37 °C. At successive time points, aliquots were removed and plated onto selective plates containing 0.2% glucose to enumerate colony-forming units (CFU).

Protein Purification—*E. coli gyrA* and *gyrB* and *V. cholerae parD*2 and *parE2* were each introduced into a modified pET28b (+) expression vector (Novagen) to yield recombinant proteins that contain a His_6 tag on their respective N termini. This modified pET28b vector encodes a tobacco etch virus protease recognition site (22). The DNA sequences of these constructs were confirmed. Proteins were expressed and purified according to a standard protocol (GE Healthcare). Briefly, 1-liter cultures of *E. coli* BL21(DE3) containing one of the expression vectors was grown at 37 °C in LB supplemented with kanamycin to an A_{600} of ~0.6, then protein expression was induced by the addition of 1 mM isopropyl-β-D-

thiogalactopyranoside (IPTG), and growth was continued for an additional 4 h at 25 °C. Then the cells were lysed in a French pressure cell, and the His-tagged proteins were purified using His-Trap nickel columns (Amersham Biosciences) on an FPLC. The column was equilibrated with binding buffer (50 mM NaH_2PO_4, pH 8.0, 500 mM NaCl. 20 mM imidazole, 10% glycerol). After washing with buffer W (50 mM NaH_2PO_4, pH 8.0, 500 mM NaCl, 20 mM imidazole, 10% glycerol), His_6-tagged proteins were eluted from the column with a 20-ml linear imidazole gradient (20–500 mM imidazole). Fractions containing pure protein (purity >90% estimated by SDS-PAGE) were pooled and dialyzed overnight at 4 °C in protein storage buffer (20 mM Tris-HCl, pH 8.0, 0.5 M NaCl, 3 mM DTT, 50% glycerol). Size-exclusion chromatography was subsequently performed for further purification of His-GyrA and His-GyrB. When purifying His-tagged versions of either GyrB or GyrA, we noticed that endogenous GyrA or GyrB, respectively, always co-purified along with the epitope-tagged subunit. This was routinely monitored with dot blots performed with anti-GyrA and anti-GyrB antibodies. These blots revealed that more GyrA co-purified with His-GyrB than GyrB with His-GyrA (data not shown).

Native ParE2 was generated by removing the N-terminal His_6 tag from purified His_6-ParE2 using AcTEV protease (Invitrogen) according to manufacturer's protocol. *Vibrio fischeri* CcdB and *E. coli* GyrA14, GyrA59 were produced as described by Dao-Thi *et al.* (23) and De Jonge *et al.* (14), respectively. *E. coli* GyrB was provided by Inspiralis Ltd. (Norwich, UK).

In Vivo Protein Interaction and Analysis—Log-phase cultures of JY302 or JY307 were grown in 0.02% arabinose and 50 μM IPTG for 2 h to induce both His_ParE2 and ParD2-myc expression. His_6ParE2 was affinity-purified using an Ni-nitrilotriacetic acid (Ni-NTA) resin (Qiagen) according to the manufacturer's instructions. Briefly, cell lysates were incubated with Ni-NTA resin equilibrated with binding buffer 50 mM NaH_2PO_4, pH 8.0, 500 mM NaCl, 10 mM imidazole for 2 h at 4 °C. Wash buffer was 50 mM NaH_2PO_4, pH 8.0, 500 mM NaCl, 20 mM imidazole, and elution buffer was 50 mM NaH_2PO_4, pH 8.0, 500 mM NaCl, 250 mM imidazole. All fractions were collected and analyzed by Western blotting. Blots were probed with anti-Myc antibody (Invitrogen) or anti-His antibody (Genetex) or anti-GyrA antibody (Inspiralis) or anti-GyrB antibody (Inspiralis).

Surface Plasmon Resonance—Surface plasmon resonance experiments were performed on a BIAcore® 2000 system (GE Healthcare). The interactions between *V. cholerae* ParE2 or *V. fischeri* CcdB and various gyrase fragments were analyzed on both CM5 and Ni-NTA chips.

Sensor Chip CM5—E. coli His-GyrA, His-GyrA14, and His-GyrB were immobilized on a CM5 sensor chip (GE Healthcare) via amine coupling. For immobilization, the system was initially primed with Hepes-buffered saline with a flow rate of 5 μl/min. The carboxylated dextran matrix was activated by a 7-min injection of a solution containing 0.2 M *N*-ethyl-*N*′-(3-diethylamino)propyl) carbodiimide and 0.05 M *N*-hydroxysuccinimide. A protein solution in 10 mM sodium acetate, pH 4.5, was then injected until the desired amount of protein was immobilized. The surface immobilization was then blocked by a 7-min injection of 1 M ethanolamine hydrochloride. Henegg lysozyme was coupled in a similar fashion in the remaining flow cell for reference subtraction. After having been coupled to the CM5 chip, His-GyrB was washed with regenerating buffer (50 mM NaOH, 1 M NaOH) before analysis. This protocol greatly reduced the amount of the co-purifying untagged GyrA subunit (data not shown). Binding experiments were performed at 25 °C in running buffer (35 mM Tris-HCl, pH 7.5, 25 mM NaCl, 5 mM $MgCl_2$, 5 mM dithiothreitol, 5% glycerol, 0.02% Tween 20) that was filtered and de-gassed before usage. The flow was set at 30 μl/min, and data were collected at 1 Hz. All analytes were dialyzed into the running buffer before analysis. Association was observed for 120 s, and dissociation was observed for 240 s. Regeneration was performed with 10 μl of regeneration buffer. The binding data were analyzed with the BIAevaluation 4.1 software (GE Healthcare), and the figures were generated with pro Fit 6.1.11 (Quantum Soft).

For the kinetic analysis on the ParE2-GyrA59 interaction (Fig. 5*G*), *E. coli* GyrA59 was immobilized on a CM5 sensor chip in a similar manner. About 1200 relative units of GyrA59 was immobilized in flow cell 2 of the chip and washed with regeneration buffer (100 mM NaOH). The surface in flow cell 1 was used as a reference and treated only with *N*-ethyl-*N*′-(3-diethylamino)propyl) carbodiimide, *N*-hydroxysuccinimide, and ethanolamine. Sensorgrams of different *V. cholerae* ParE2 concentrations (3.9 nM, 7.8 nM, 15.6 nM, 31.25 nM, 62.6 nM, 125 nM, 250 nM, 500 nM, 1 μM, 2 μM) plus a 0 concentration (injection of running buffer) were collected in duplicate. The flow was set at 5 μl/min, and data were collected at 2 Hz. This low flow rate was chosen based on the small quantity of ParE2 available; purifying large quantities of the protein was not feasible given its toxicity. Mass transport phenomena are likely at play under these conditions, and thus, the reported values for k_{on}, k_{off}, and K_D should be regarded as apparent.

All analytes were dialyzed into the running buffer before analysis. Association was observed for 500 s and dissociation was observed for 300 s. Regeneration was performed with 10 μl of regeneration buffer. The sensorgrams were fitted to a heterogeneous ligand model according to the equations below after subtraction of the reference and zero concentration data, which provided the kinetic parameters for the ParE2-GyrA59 interaction.

$$\text{Ligand 1: } \frac{d[AB_1]}{dt} = k_{on1}[A][B_1] - k_{off1}[AB_1] \qquad \text{(Eq. 1)}$$

$$\text{Ligand 2: } \frac{d[AB_2]}{dt} = k_{on2}[A][B_2] - k_{off2}[AB_2] \qquad \text{(Eq. 2)}$$

In this model *A* denotes the analyte, and *B* denotes the ligand.

Sensor Chip NTA—E. coli GyrA, GyrA14, GyrA59, and GyrBA were immobilized on a BIAcore® Ni-NTA sensor chip (GE Healthcare) via their N-terminal hexahistidine tags as described (24). Binding experiments were performed as described above with a different running buffer (35 mM HEPES pH 7.5, 25 mM NaCl, 5 mM $MgCl_2$, 0.005% Tween 20). To ensure that the chip was free of any ligand, 20 μl of regeneration

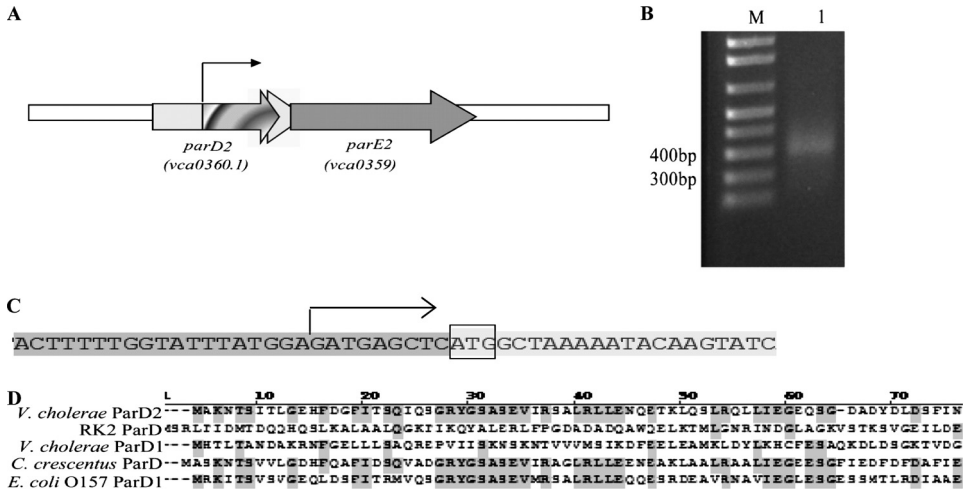

FIGURE 1. **Organization of the *V. cholerae parDE2* locus.** A, shown is a schematic representation of the *parDE2* region in the *V. cholerae* N16961 chromosome. The *white arrow* represents the original *vca0360* ORF as previously annotated (26), and the *light gray arrow* represents the *vca0360.1* ORF as annotated in Bocs *et al.* (27). The *thin arrow* represents the predicted *parD2* promoter based on the 5′ rapid amplification of cDNA ends. *B*: *lane M*, 1-kb plus marker; *lane 1*, specific PCR product from the 5′ rapid amplification of cDNA ends experiment. *C*, the start of the *parD2* transcript, represented by the *arrow*, was determined by sequencing the PCR shown in *B*. The *parD2* translational start site, as predicted by Bocs *et al.* (27), is shown with the *box around the ATG*. *D*, alignments of the predicted amino acid sequences of *vca0360.1* (*V. cholerae* ParD2) with the indicated chromosome- and plasmid (RK2)-encoded ParD sequences are shown.

buffer (10 mM HEPES, pH 8.3, 150 mM NaCl, 350 mM EDTA, 0.005% Tween 20) was passed over the flow cells at 5 μl/min. This was followed by a 20-μl injection of the activation buffer (500 μM $NiSO_4$, 35 mM HEPES, pH 7.5, 25 mM NaCl, 5 mM $MgCl_2$, 0.005% Tween 20) in flow cell 2 at 10 μl/min. The ligands His-GyrA14, His-GyrA59, His-GyrBA, and His-GyrA were, respectively, immobilized to the chip by injecting 10, 10, 10, and 50 μl of a 7 μg/ml solution at 20 μl/min followed by a dissociation time of 100 s. The analytes were injected at a volume of 30 μl at 20 μl/min followed by a dissociation time of at least 400 s. Regeneration was subsequently performed by injecting 40 μl of regeneration buffer at 10 μl/min.

For the interaction between *V. cholerae* ParD2 and ParE2, N-terminal His-tagged ParD2 was non-covalently coupled to a Ni-NTA chip by injecting 10 μl of a 7 μg/ml solution at 20 μl/min followed by a dissociation time of 100 s. The rest was performed as described for the ParE2-gyrase interaction on the Ni-NTA chip.

Gyrase Activity Assays—DNA gyrase supercoiling, relaxation, and cleavage assays were performed essentially as described (25). Substrates for these assays were 3.5 nM relaxed pBR322, 1.02 nM supercoiled pCB182, or 4.82 pM *V. cholerae* chromosomal DNA. For supercoiling and cleavage assays, the reaction buffer was 35 mM Tris-HCl, 24 mM KCl, 4 mM $MgCl_2$, 2 mM DTT, 1.8 mM spermidine, 1 mM ATP, 6.5% glycerol, and 0.1 mg/ml BSA. For holoenzyme relaxation assays, ATP and spermidine were omitted from the assay buffer, and for $A59_2B_2$ relaxation assays, ATP was included. 1 unit of DNA gyrase (30 nM) (New England Biolabs) or 100 nM $A59_2B_2$, 1.88 μM ParE2, 2.25 μM ParD2, and 0.5 mM nalidixic acid (Sigma) were used as indicated. Both supercoiling and cleavage reactions were carried out at 37 °C for 1 h, whereas relaxation reactions were performed at 30 °C for 3.5 h. The reactions were stopped with 50 μg/ml proteinase K and 1% SDS. The DNA was precipitated with phenol:chloroform: isoamyl alcohol (25:24:1) (Invitrogen) before it was loaded on to 1% agarose gels and electrophoresed in the absence of ethidium bromide.

RESULTS

The V. cholerae parD2 Locus Was Mis-annotated—The predicted *V. cholerae* ParE2 amino acid sequence exhibits 29% sequence identity with RK2-ParE. In contrast, the predicted ParD2 sequence is only 12% identical to RK2 ParD. However, two different annotations of the *V. cholerae parD2* locus have been reported. In the original annotation of the genome of *V. cholerae* El Tor strain N16961, the *parD2* locus (*vca0360*) was predicted to encode a protein of 153 amino acids (26). In a bioinformatics study re-annotating microbial genomes, Bocs *et al.* (27) predicted that *parD2* is actually a shorter ORF, *vca0360.1*, embedded within *vca0360* (Fig. 1*A*). We used 5′ rapid amplification of cDNA ends to experimentally investigate the *parD2* transcription start site. This analysis revealed that the start of *parD2* transcription initiated 182 nucleotides 3′ of the annotated *vca0360* translational start site, 11 bp 5′ of the translation start site predicted by Bocs *et al.* (27) (Fig. 1). Additional analyses suggest that there is a recognizable and functional promoter upstream of this transcription start site (data not shown). The predicted VCA0360.1 ORF yields a protein of 80 amino acids that exhibits up to 67% sequence similarity to other chromosome-encoded ParDs and 24% identity to the RK2 plasmid-encoded ParD (Fig. 1*D*). In contrast, the predicted VCA0360 amino acid sequence exhibited less similarity to other ParD2 proteins. Together, these observations strongly suggest that *vca0360.1* encodes *V. cholerae* ParD2, and we used this *parD2* annotation for the studies described below.

ParE2 Is Toxic to Both V. cholerae and E. coli, and Its Toxicity Can Be Ameliorated by ParD2—We constructed plasmid-borne inducible versions of *parE2* and *parD2* to test if these *V. cholerae* genes encode a functional toxin/antitoxin pair. Expression of *parE2* from pBAD-E2 is induced by arabinose,

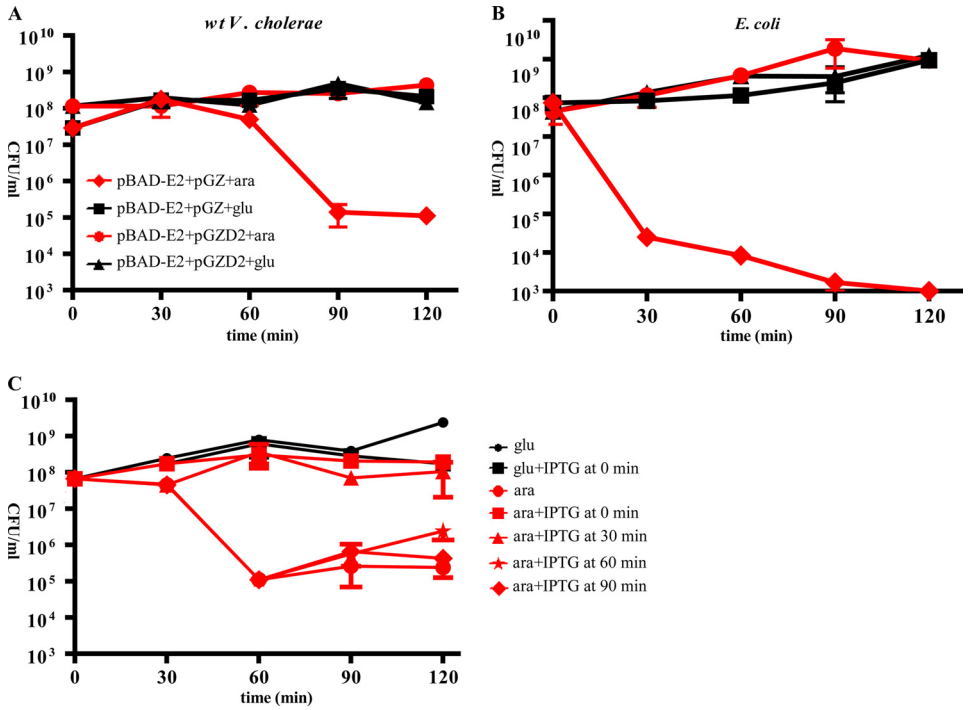

FIGURE 2. **Effect of ParE2 and ParD2 on *V. cholerae* and *E. coli* viability.** *V. cholerae* N16961 (*A*) and *E. coli* BW27784 (*B*) contained a plasmid-borne, arabinose-inducible *parE2* (pBAD-E2) and either an empty vector (pGZ, *diamonds* and *squares*) or the vector harboring *parD2* under control of its native promoter (pGZ-D2, *circles* and *triangles*). All cultures were grown in LB supplemented with 0.2% glucose at 37 °C until an A_{600} of ~0.3, washed and resuspended in either LB plus 0.2% glucose (*glu*) (*black squares* and *triangles*) or LB plus 0.02% arabinose (*ara*) (*red diamonds* and *circles*). CFU were enumerated at the indicated time points. *C*, *E. coli* BL21 (pBAD-E2, pET-D2), (JY307), harbors plasmids with arabinose-inducible *parE2* and IPTG-inducible *parD2*. Cultures were grown in LB supplemented with 0.2% glucose until an A_{600} of ~0.3, washed and resuspended in either LB plus 0.2% glucose (*glu*) or glucose plus 50 μM IPTG (*black squares* and *circles*) or LB plus 0.02% arabinose (*ara*) (*red shapes*). IPTG (50 μM) was added at the indicated time points after the addition of arabinose. CFU were enumerated at the indicated time points.

whereas expression of *parD2* from pGZ-D2 is constitutive and driven by its endogenous promoter. The *parE2* expression construct was introduced along with either pGZ-D2 or a vector control into wild type El Tor *V. cholerae* strain N16961 and *E. coli* BW27784. Induction of *parE2* expression in the absence of the *parD2* expression construct was highly toxic in both strains. After *parE2* induction, the number of CFU in cultures was reduced by ~3–5 orders of magnitude relative to the number in cultures in which *parE2* expression was repressed with glucose (Fig. 2, *A* and *B*, *red diamonds versus black squares*). The rapidity and magnitude of the reduction in CFU after induction of *parE2* expression were even more dramatic in *E. coli* BW27784 than in *V. cholerae*, perhaps because this *E. coli* strain has a constitutive arabinose transporter and does not exhibit inducer exclusion (28), and ParD2 in the wild type *V. cholerae* strain may partially neutralize the effect of ParE2. Notably, no toxicity after *parE2* induction was observed in any strain containing pGZ-D2. Collectively, these data suggest that *parE2* encodes a toxin whose target is conserved between *V. cholerae* and *E. coli* and whose activity can be neutralized by ParD2.

We also tested whether ParD2 could reverse ParE2 toxicity *in vivo*. For these experiments we used *E. coli* BL21 containing pBAD-E2 and pET-*parD2* (JY307), which enabled inducible expression of both proteins. The strain was initially cultured in glucose to repress *parE2* expression. As described above, induction of *parE2* expression in the absence of *parD2* induction reduced the plating efficiency of this strain by several orders of magnitude, whereas induction of *parE2* expression when *parD2* was produced simultaneously did not impair plating efficiency (Fig. 2*C*). Induction of *parD2* expression 30 min after induction of *parE2* also did not reduce the number of CFU. However, when *parD2* expression was initiated 60 or 90 min after induction of *parE2*, little or no neutralization of ParE2 toxicity was detected (Fig. 2*C*, *red stars* and *red diamonds*, respectively). These results suggest that ParD2, unlike several previously characterized antitoxins, such as RelE (29), may be unable to reverse the toxicity of its cognate toxin.

ParE2 and ParD2 Interact—Protein antitoxins typically neutralize their cognate toxins by binding to them and inhibiting their ability to interact with their respective cellular targets (30–33), We investigated whether ParD2 interacts with ParE2 *in vivo* by testing whether epitope-tagged versions of these proteins would co-purify from *E. coli* BL21 co-expressing ParE2-Myc and His-ParD2 (JY307). The N-terminal His-tagged ParD2 was affinity-purified from lysates of JY307 using Ni-NTA resin. After washing, protein bound to the resin was eluted with increasing concentrations of imidazole. The eluted fractions were then immunoblotted with anti-His and anti-Myc antisera. As seen in Fig. 3*A*, these Western blots revealed that ParE2-Myc was purified along with His-ParD2. A mock purification using lysate from cells expressing ParE2-Myc but not His-ParD2 revealed that ParE2-Myc did not bind to the Ni-NTA resin in the absence of His-ParD2 (Fig. 3*B*). Together, these observations suggest that ParE2 is present in a complex containing ParD2, but they do not establish that

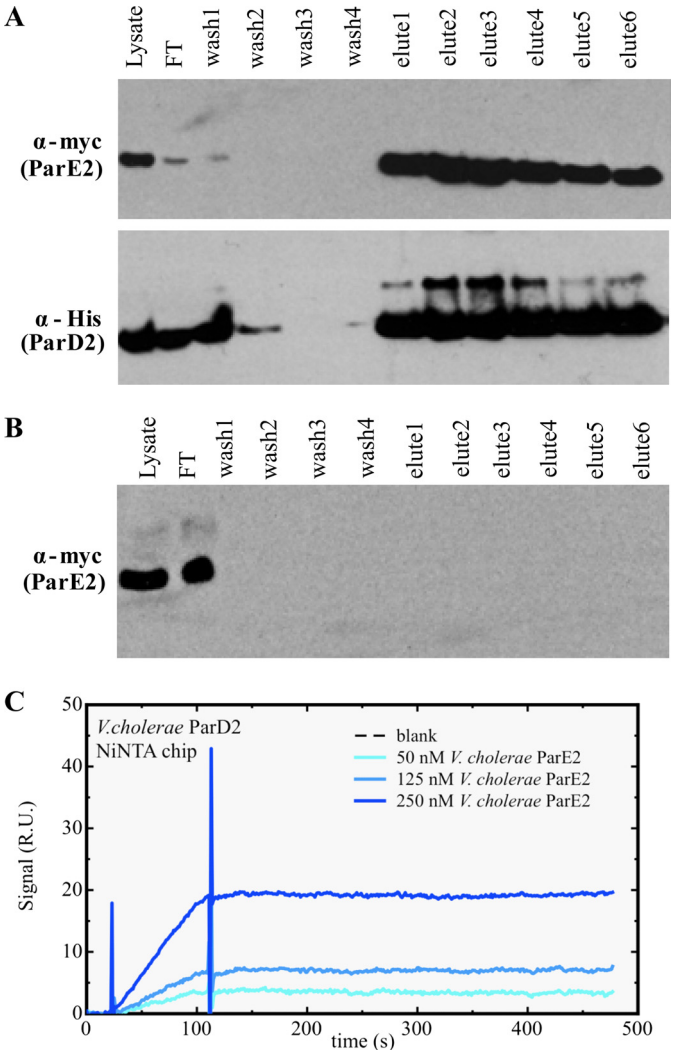

FIGURE 3. **Co-purification of Myc tagged ParE2 with His-tagged ParD2.** *A*, His-ParD2 from JY307, *E. coli* BL21 co-expressing His-ParD2 and ParE2-Myc (lysate) was affinity-purified using Ni-NTA resin. The starting lysate flowthrough (*FT*), washes, and eluted fractions were analyzed by Western blotting with anti-His and anti-Myc antibodies. *B*, cell lysate from JY281, *E. coli* DH5α-expressing ParE2-Myc were processed as in *A* and then analyzed using anti-Myc antibody. *C*, His-tagged ParD2 (~50 relative units (*R.U.*) was coupled to a Ni-NTA chip, and native ParE2 was injected at the indicated concentrations, expressed in terms of monomer.

there is direct contact between these proteins. However, surface plasmon resonance (SPR) assays using purified His-ParD2 and untagged ParE2 demonstrated that these proteins physically interact and form a stable complex (Fig. 3*C*).

ParE2 Interacts with DNA Gyrase—Even though ParE2 only exhibits a modest degree of sequence identity to the ParE encoded by plasmid RK2, we explored whether it has the same cellular target as the plasmid-encoded toxin DNA gyrase. First, we tested whether we could detect an association between ParE2 and gyrase *in vivo*, as described above for His-ParD2 and ParE2-Myc. Western blotting of proteins purified from *E. coli* BL21 expressing His-ParE2 (JY302) revealed that fractions containing affinity-purified His-ParE2 also contained GyrA and GyrB (Fig. 4*A*). GyrA and GyrB were not detected in control purifications performed using lysates of BL21-expressing His-ParD2 (JY262), indicating that they do not bind non-specifically to the affinity matrix (Fig. 4*B*). These results suggest that ParE2 is part of a complex containing GyrA and GyrB *in vivo*. Because GyrA and GyrB form a tight tetramer, it is not surprising that both gyrase subunits co-eluted with ParE2.

To explore if ParD2 could prevent ParE2 interactions with gyrase, we overexpressed His-ParD2 along with ParE2. In this context, no GyrA or GyrB co-purified along with ParD2 and ParE2 (Fig. 4*C*), suggesting that when ParE2 is bound to ParD2, the toxin cannot interact with gyrase.

ParE2 Binds to GyrA—To further characterize the interactions of ParE2 and gyrase, the binding of ParE2 to gyrase and the individual gyrase subunits was probed using SPR. In these experiments we compared the interaction of ParE2 with different regions of DNA gyrase from *E. coli* immobilized on BIAcore sensor chips. As a control, we examined the binding of the *V. fischeri* CcdB toxin, which is known to bind to GyrA (34, 35), to the same chips. Initially, the binding of the toxins to GyrBA was examined. A His-GyrB-GyrA complex was non-covalently coupled to a Ni-NTA sensor chip to probe the interactions between the toxins and GyrBA. As seen in Fig. 5*A*, *V. fischeri* CcdB and *V. cholerae* ParE2 both bound to GyrBA.

Next, interactions between ParE2 and the individual gyrase subunits were examined. As shown in Fig. 5*B*, neither ParE2 nor CcdB interacted with GyrB alone. However, an association between GyrB and GyrA was observed (Fig. 5*B*, *green line*), suggesting that the GyrB bound to the chip was properly folded. In addition, we observed that ParE2, like CcdB, bound to chips coated only with His-GyrA (Fig. 5*C*). Together, these data indicate that the copurification of GyrB along with affinity-purified ParE2 (Fig. 4) was due to an indirect association of these proteins that was mediated by GyrA.

ParE2 Binds to a Different Site on GyrA than CcdB—To gain insight into the ParE2 target within GyrA, we made use of previously characterized fragments of this enzyme. We observed that ParE2, like CcdB, binds to GyrA59, a 59-kDa fragment that includes the N-terminal amino acid residues 2–523 but lacks the C-terminal DNA-wrapping domain (Fig. 5*D*). Model-based analysis of the sensorgrams recorded during the multicycle analysis of the ParE2-GyrA59 interaction revealed that the binding of ParE2 to GyrA59 is not monophasic; instead, two binding events occur in parallel. The simplest model providing a reasonable fit to the data is a heterogeneous ligand model. This model has a χ^2 of 1.84 and indicates a high affinity for the ParE2-GyrA59 interaction with a K_D between ~20 pM and 10 nM (Fig. 5*G*). The heterogeneity in binding of ParE2 by GyrA59 was most likely introduced by the immobilization method. Such heterogeneity was also observed in the interaction of covalently coupled GyrA59 with CcdB (51).

Although ParE2 and CcdB both bind to GyrA59 with similar high affinity, the toxins differed in their ability to bind a GyrA fragment known as GyrA14 (amino acids 363–497), which mediates the dimerization of GyrA monomers. SPR revealed no interaction between ParE2 and this fragment, whereas, as previously reported, binding of CcdB was apparent, indicating that the two toxins recognize distinct regions

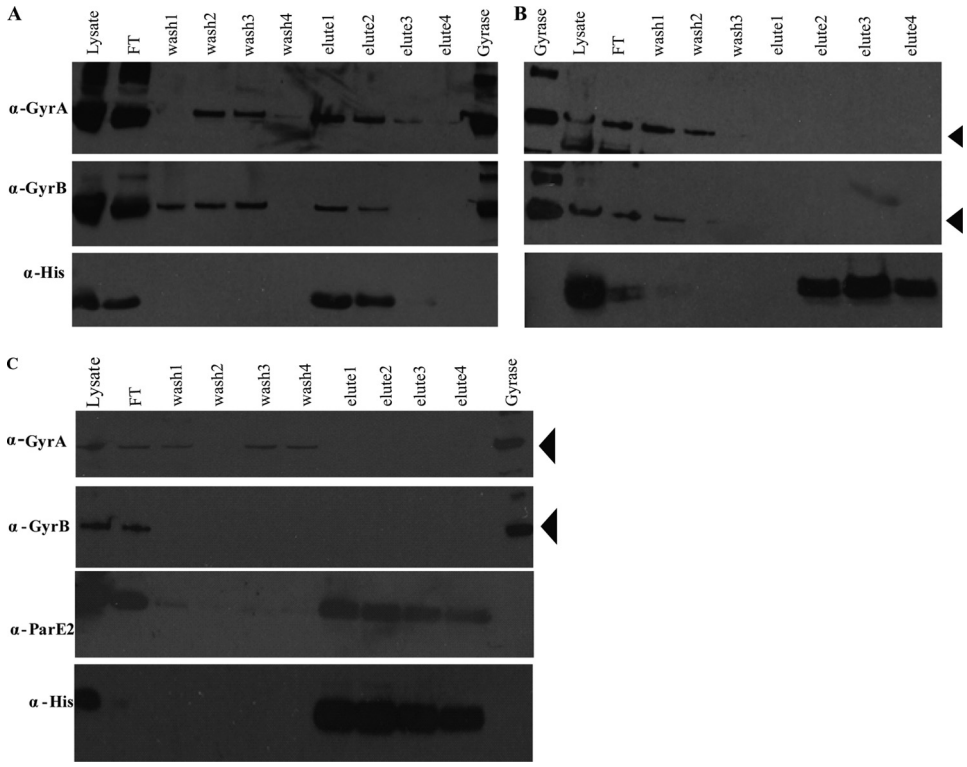

FIGURE 4. **Co-purification of GyrA and GyrB with His-ParE2.** Cell lysates from *E. coli* BL21(DE3) expressing His-ParE2 (JY302) (*A*) or expressing His-ParD2(JY262) (*B*) or *E. coli* BL21 co-expressing His-ParD2 and ParE2-Myc (JY307) (*C*) were incubated with Ni-NTA resin, washed, and then eluted with imidazole. The initial lysates flowthrough (*FT*), washes, and eluted fractions were electrophoresed on polyacrylamide gels and then analyzed by Western blotting with anti-GyrA, anti-GyrB anti-His, and anti-ParE2 antibodies as indicated. Purified *E. coli* gyrase was used as the control. The positions of GyrA or GyrB are indicated with *arrows*.

within GyrA (31, 36, 37) (Fig. 5*E*). Further support for this conclusion was provided by the observation that a Ni-NTA-GyrA chip whose binding to CcdB is fully saturated can still readily bind ParE2 (Fig. 5*F*).

Furthermore, *in vivo* studies also indicated that ParE2 and CcdB have distinct targets within GyrA. Consistent with previous reports, expression of GyrA14 protected cells from the toxicity of CcdB, likely by titrating CcdB from its cellular target (37) (supplemental Fig. S1). In contrast, GyrA14 did not prevent ParE2 toxicity. Even in the presence of GyrA14, more than a 10-fold reduction in CFU was observed after induction of ParE2 expression (supplemental Fig. S1*A*). These findings provide strong support for the idea that ParE2 binds to a different domain of GyrA than CcdB. As expected, ParE2 toxicity was neutralized by ParD2 in this system, but ParD2 did not protect cells from the toxicity of *V. fischeri* CcdB (supplemental Fig. S1*B*).

ParE2 Stabilizes Gyrase-DNA Cleavage Intermediates—Studies on quinolone antibiotics (*e.g.* nalidixic acid (Nal)), CcdB, and RK2-encoded ParE revealed that these agents all inhibit the gyrase catalytic cycle by stabilizing DNA-gyrase cleavage intermediates. Such cleaved intermediates are readily detectable on agarose gels after reaction mixtures of gyrase, DNA, and toxins are treated with SDS and proteinase K (38, 39). We used a similar protocol to test whether ParE2 also stalls the gyrase-DNA cleavage complex using purified *E. coli* gyrase, ParE2, and *V. cholerae* chromosomal DNA as a substrate. In this assay Nal caused gyrase-dependent cleavage of the chromosomal DNA substrate (Fig. 6, *lanes 3* and *4*), as expected. The addition of ParE2 to gyrase also resulted in the formation of cleaved DNA (Fig. 6, compare *lane 2 versus 7*), but ParE2 did not cleave the DNA on its own (Fig. 6, *lane 6*). Together, these observations strongly suggest that ParE2, like Nal, stabilizes gyrase-DNA cleavage complexes. Similar results were also obtained when negatively supercoiled plasmid DNA was used as the substrate (data not shown).

We carried out similar assays to test whether ParD2 could prevent and/or reverse ParE2 stabilization of gyrase-DNA cleavage complexes. When ParD2 was mixed with ParE2 before their addition to gyrase and DNA, near complete neutralization of ParE2 activity was observed (Fig. 6, compare *lane 9 versus 7*, and supplemental Fig. S2, *lane 8*). However, when ParD2 was added simultaneously with ParE2 to the reaction, less complete neutralization was observed (supplemental Fig. S2, *lane 6*). Finally, when ParD2 was added 30 min after ParE2, relatively little neutralization of the ParE2 effect was detected (supplemental Fig. S2, *lane 7*). We also found that ParE2-GyrA59 complex immobilized on the sensor chip could not be disrupted by ParD2 (data not shown). Together, these findings support the idea that ParD2 is unable to rescue ParE2-poisoned gyrase, which are consistent with the observation that ParD2 could not reverse ParE2 toxicity *in vivo* (Fig. 2*C*). Thus, ParD2 appears to differ from RK2 ParD (13) and CcdA (25), which can rejuvenate ParE- or CcdB-poisoned gyrase, respectively.

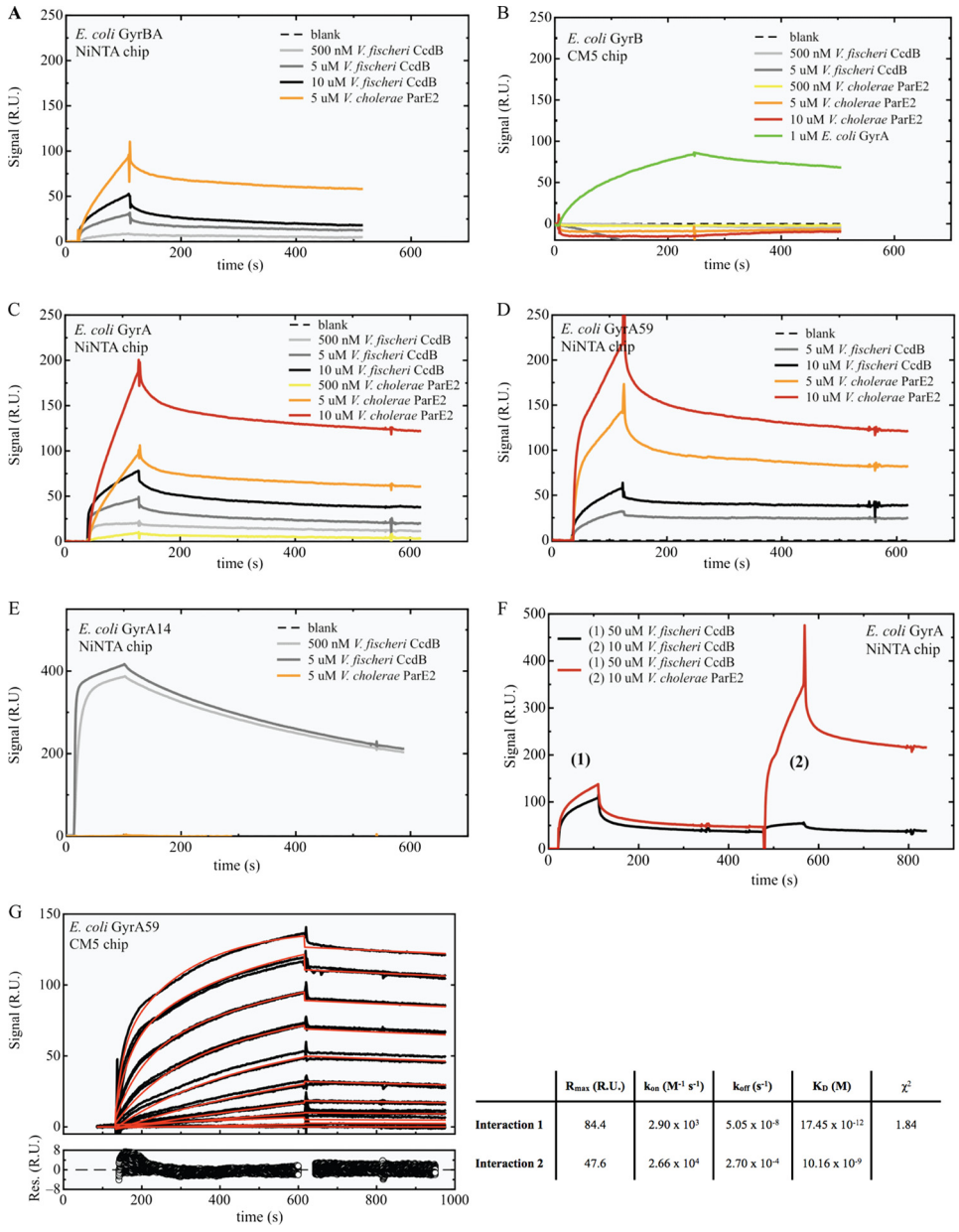

	R_{max} (R.U.)	k_{on} (M^{-1} s^{-1})	k_{off} (s^{-1})	K_D (M)	χ^2
Interaction 1	84.4	2.90×10^{3}	5.05×10^{-8}	17.45×10^{-12}	1.84
Interaction 2	47.6	2.66×10^{4}	2.70×10^{-4}	10.16×10^{-9}	

FIGURE 5. **SPR measurements of interactions between *V. cholerae* ParE2 or *V. fischeri* CcdB and gyrase.** GyrBA (~200 relative units (*RU*)) (*A*), GyrA (~150 RU) (*C*), GyrA59 (~600 RU) (*D*), and GyrA14 (~400 RU) (*E*) were non-covalently coupled to a Ni-NTA chip, whereas GyrB (~1800 RU) (*B*) was covalently coupled to a CM5 chip. The analytes were injected over the immobilized ligands at the indicated concentrations, expressed in terms of monomer. *F*, *V. fischeri* CcdB was injected at a concentration of 50 μM to saturate the CcdB binding site on GyrA. After a dissociation time of 200 s, ParE2 was injected at a concentration of 10 μM. A control experiment with a second CcdB (10 μM) injection showed that all CcdB binding sites are saturated after the first CcdB injection. *G*, shown is kinetic analysis of the interaction between *V. cholerae* ParE2 and *E. coli* GyrA59. The *top graph* displays the sensorgrams at different ParE2 concentrations (0 nM, 3.9 nM, 7.8 nM, 15.6 nM, 31.25 nM, 62.5 nM, 125 nM, 250 nM, 500 nM, 1 μM, 2 μM), which were collected in duplicate and are shown in *black*. The *red lines* represent the best fit of the model function (heterogeneous ligand model) to the experimental curves. The residuals of the fitting procedure are shown in the *bottom graph*. Model-based analyses of the sensorgrams recorded during the multicycle analysis of the ParE2-GyrA59 interaction indicates that the binding of ParE2 to GyrA59 is not monophasic and that two binding events occur in parallel. Fitting with a simple 1:1 Langmuir binding model does not result in acceptable residuals ($\chi^2 = 22.4$). The simplest model providing a reasonable fit to the data is a heterogeneous ligand model, resulting in a χ^2 of 1.84. In aggregate, analysis of this data set reveals a very high affinity for the ParE2-GyrA59 interaction with a K_D between ~20 pM and 10 nM.

ParE2 Inhibits Gyrase Supercoiling Activity in an ATP-dependent Manner—We further characterized the ParE2 effect on gyrase utilizing additional *in vitro* assays of gyrase activity, as earlier studies of RK2 ParE did not specifically address whether this plasmid-encoded toxin inhibited gyrase-mediated DNA relaxation and/or supercoiling (13). Gyrase has previously been shown to relax supercoiled plasmid DNA and to introduce supercoils into relaxed plasmids *in vitro*. The first reaction proceeds relatively slowly but is ATP-independent, whereas the latter reaction requires ATP (25, 38, 39). Both can be interrupted by agents such as CcdB and quinolone antibiotics, which stabilize gyrase-DNA reaction intermediates.

We used plasmid DNA substrates and purified *E. coli* gyrase to investigate whether ParE2 interferes with gyrase-catalyzed supercoiling and/or relaxation of DNA. Using a relaxed

plasmid substrate, we found that ParE2, like Nal and CcdB, inhibited introduction of supercoils by gyrase with an IC_{50} of ~1.2 μM (Fig. 7*A*, compare *lanes 2*, *4*, and *5*, and supplemental Fig. S3), a similar value as CcdB (25). ParE2 effect could be blocked by preincubation of this protein with ParD2 (Fig. 7*A*, *lane 8*), consistent with the ParD2 previously noted role as an antitoxin *in vivo* and *in vitro*. In contrast, ParE2 and Nal had distinct effects upon relaxation of plasmid DNA (Fig. 7*B* and supplemental Fig. S4). The addition of a range of ParE2 concentrations had no effect upon gyrase-mediated relaxation of a supercoiled substrate (Fig. 7*B*, compare *lane 2* and *6*, and supplemental Fig. S4, compare *lanes 3–7*), whereas the addition of Nal (Fig. 7*B*, *lane 4*) resulted in accumulation of cleaved DNA intermediates (Fig. 7*B*, *lane 4*), as previously described (40). Furthermore, no or minimal inhibition of DNA relaxation was detected during a time course extending from 0 to 6 h in the presence of ParE2 (data not shown). These data suggest that ParE2, like Nal, can inhibit gyrase activity but that its mechanism of action differs. In particular, ParE2 appears to lack the capacity to block gyrase-mediated relaxation of DNA.

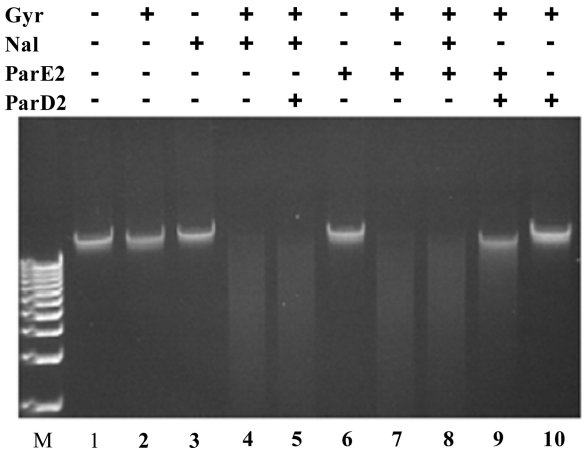

FIGURE 6. **Effect of ParE2 and ParD2 on cleavage of chromosomal DNA by gyrase.** *In vitro* reactions with chromosomal DNA, gyrase, ParE2, and ParD2 were carried out as described under "Experimental Procedures." *M* indicates 1 kb plus DNA ladder.

As the supercoiling assay, unlike the relaxation assay, is performed in the presence of ATP, we assessed whether the presence of nucleotide was important for ParE2 activity. For these assays we used a chromosomal DNA substrate (which is expected to mostly consist of linear DNA molecules). The addition of gyrase alone to this substrate either in the absence or presence of ATP had no discernible effect on its integrity, as expected when gyrase-mediated cleavage is followed by religation (Fig. 8). The addition of Nal resulted in accumulation of cleavage intermediates; as previously reported (38), this disruption of the gyrase reaction cycle was not dependent on ATP hydrolysis, although it did appear to be enhanced by the presence of nucleotide (Fig. 8, compare *lanes 4–7*). In contrast, the addition of ParE2 to reactions containing gyrase resulted in accumulation of cleavage intermediates only in the presence of ATP. No cleavage was detected when ATP was replaced by the non-hydrolyzable analog ATPγS or by GTP. Thus, although ParE2, like Nal and other gyrase poisons, can stabilize DNA-gyrase cleavage intermediates, the ParE2 effect appeared to be dependent upon gyrase binding to and hydrolyzing ATP.

An alternative explanation of the requirement for ATP for ParE2 toxicity is that the activity of ParE2 itself could depend on ATP. To exclude this possibility, we used a reconstituted gyrase ($A59_2B_2$) containing a truncated GyrA that lacks the C-terminal 33-kDa DNA-wrapping domain of GyrA (18). The $A59_2B_2$ complex cannot supercoil DNA, even in the presence of ATP, but it retains the ability to relax negatively supercoiled DNA. Consequently, use of this enzyme allowed the effect of ParE2 on relaxation of a supercoiled substrate to be assessed in the presence of ATP (17). In this assay, the $A59_2B_2$ complex could convert nearly all of a supercoiled plasmid to a relaxed form (supplemental Fig. S5, *A*, *lane 1 versus* 2, and *B*, *lane 1 versus* 3). Inclusion of Nal in the reaction markedly inhibited $A59_2B_2$ relaxation of the plasmid (supplemental Fig. S5*A*, *lanes 3* and *4*), similar to previous reports where ciprofloxacin was used (25). In contrast, a range of ParE2 concentrations did not inhibit $A59_2B_2$ activity even in the presence of ATP (supplemental Fig. S5 *A*, *lane 6*, and *B*, *lanes 4–7*). These findings buttress the conclusion that ParE2 lacks the ability to

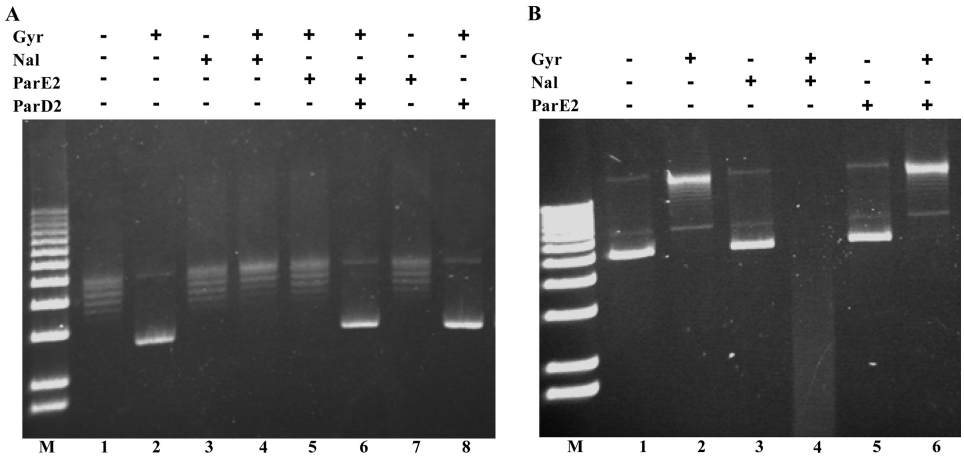

FIGURE 7. **The effect of ParE2 on gyrase supercoiling (*A*) and relaxation (*B*) of plasmid DNA substrates.** The reactions were performed as described under "Experimental Procedures" except in *B* the reaction was stopped with SDS and proteinase K. In *A*, the substrate was relaxed pBR322 DNA, and in *B* the substrate was negatively supercoiled pCB182. *M* indicates 1Kb plus DNA ladder.

block gyrase-mediated relaxation of DNA supercoils and argue against the possibility that ATP is required to convert ParE2 to an active form. Furthermore, these findings provide additional evidence that the ParE2 mechanism is distinct from those of quinolones and CcdB, both of which inhibit $A59_2B_2$ activity (25).

Gyrase Mutants That Confer Resistance to Known Gyrase Toxins Do Not Confer Resistance to ParE2—To continue to explore how ParE2 inhibits gyrase, we expressed ParE2 in a variety of *E. coli* strains harboring gyrase alleles that confer resistance to antibiotics and toxins that poison this enzyme.

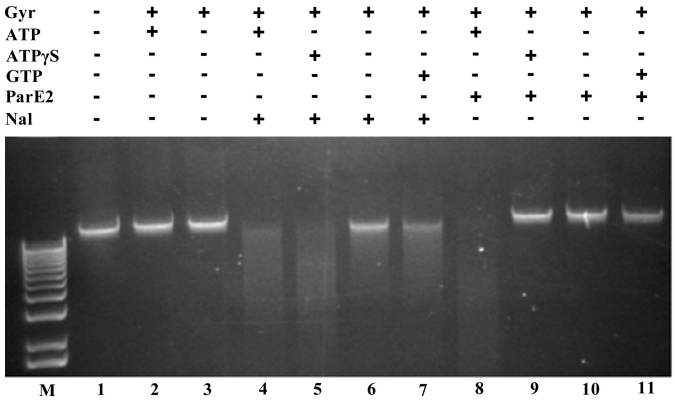

FIGURE 8. **Requirement for ATP hydrolysis in ParE2 stabilization of gyrase-DNA cleavages.** The reactions were carried out as described under "Experimental Procedures" using *V. cholerae* chromosomal DNA as substrate. 1 mM ATP, ATPγS, or GTP were used in these reactions. 5 μM ParE2 or 1 mM nalidixic acid were included as indicated. *M* indicates 1 kb plus DNA ladder.

Strains harboring *gyrB* mutations conferring resistance to coumermycin A_1 and microcin B17 were sensitive to ParE2 (data not shown). This was an expected result, as our findings indicated that ParE2 targets GyrA. Our observations presented above also suggest that ParE2 targets a different part of GyrA than CcdB. Consistent with this idea, DB3.1, a strain containing the CcdB-resistant *gyrA* R462C, was also sensitive to ParE2 (Fig. 9). Finally, all of the strains harboring *gyrA* alleles conferring resistance to Nal were sensitive to ParE2. In aggregate, these observations suggest that ParE2 poisons gyrase via a mechanism that is distinct from previously described agents that target this essential enzyme.

DISCUSSION

Our findings revealed that the *parDE2* locus found in the superintegron of *V. cholerae* chromosome II encodes a functional proteic TA pair. Overexpression of ParE2 markedly inhibited growth of *V. cholerae* as well as *E. coli*, indicating that ParE2 toxicity is not restricted to *V. cholerae* and that the cellular target of ParE2 is conserved in both organisms. The *parD2* ORF was mis-annotated in the *V. cholerae* genome, but expression of the correct *parD2* ORF neutralized ParE2 toxicity. ParD2 co-purified with ParE2, and direct interactions between the proteins were detected with SPR. However, ParD2 appears to function in a different fashion than many other antitoxins, as ParD2 could prevent but not reverse ParE2 toxicity. ParE2, like plasmid RK2-encoded ParE, CcdB, microcin B17, and quinolone and coumarin antibiotics, targets DNA gyrase. We found that ParE2, like CcdB and quinolones, tar-

E. coli strain	genotype	ParE2 sensitive
MG1655	WT	+
HB101	WT	+
MLS83L	*gyrA* S83L (Nal^r)	+
MLD87G	*gyrA* D87G (Nal^r)	+
UB1005	*gyrA* 37 (Nal^r)	+
JRG902	*gyrA* 39 (Nal^r)	+
KL385	*gyrA* 49 (Nal^r)	+
JF238	*gyrA* 91 (Nal^r)	+
EWH321	*gyrA* 99 (Nal^r)	+
MC301	*gyrA* 208 (Nal^r)	+
DC403	*gyrA* 216 (Nal^r)	+
CY288	*gyrA* 220 (Nal^r)	+
Q818	*gyrA* 222 (Nal^r)	+
CAG12177	*gyrA* 261 (Nal^r)	+
LCB263	*gyrA* 271 (Nal^r)	+
MN1	*gyrA* 283 (Nal^r)	+
DB3.1	*gyrA* R462C ($CcdB^r$)	+

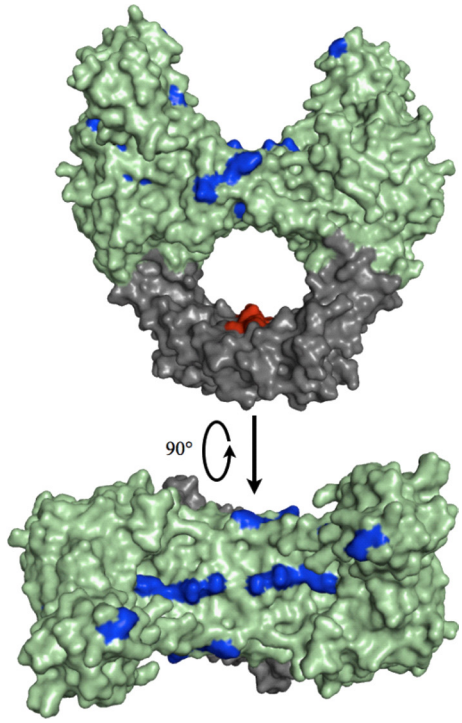

FIGURE 9. **Strains bearing gyrase alleles conferring resistance to several gyrase toxins remain sensitive to ParE2.** In *A*, the strains indicated were tested for their resistance to ParE2 after the toxin was expressed from pBAD-E2. Strains were scored as sensitive if there was attenuated growth after induction of ParE2 expression with arabinose. In *B*, the mutations listed in *A* were mapped onto the crystal structure of *E. coli* GyrA59 colored in *green* (PDB entry 1AB4 (52). GyrA14 is shown in *dark gray*, and the *red patches* correspond to the residues involved in the interaction between CcdB and GyrA (Gln-456, Asp-460, Arg-462, Gln-464). The residues conferring resistance to quinolones when mutated are colored *blue*. This figure was generated using MacPyMOL (DeLano Scientific, Ltd.).

gets GyrA and stabilizes the DNA-gyrase cleavage complex. However, ParE2, in contrast to quinolones and CcdB, did not bind to GyrA14 and required ATP hydrolysis to stabilize gyrase cleavage intermediates. Also unlike quinolones and CcdB, ParE2 only interferes with gyrase supercoiling; its ability to relax DNA is apparently unaffected. Together, these findings suggest that ParE2 may only gain access to its target site(s) on GyrA at a particular stage of the supercoiling reaction, possibly after DNA wrapping and ATP hydrolysis. Finally, a set of strains resistant to a variety of known gyrase inhibitors all exhibited sensitivity to ParE2. Thus, taken together, our findings strongly suggest that ParE2 and most likely its many plasmid- and chromosome-encoded homologues inhibit gyrase in a different manner than previously described agents that poison this essential enzyme.

ParD2 Action and Its Physiological Implications—The interaction of ParD2 with ParE2 appears to be unusual. Our findings indicate ParD2, like other antitoxins, binds to its cognate toxin ParE2. However, unlike several antitoxins, including RK2 ParD, and F-plasmid CcdA (13, 41), *V. cholerae* ParD2 appears to be unable to reverse ParE2 inhibition of gyrase activity (Fig. 6). Structural studies have revealed that at least some antitoxins interact with their cognate toxins through direct binding of a disordered region present in the antitoxin C termini. As a consequence of such interactions, the disordered region reorganizes into a well defined structure, and conformational changes occur in the toxin, distorting the binding site for the cellular target (42–44). Recently, the crystal structure of the *Caulobacter crescentus* ParD1-ParE1 complex was reported (45). Based on this structure, Dalton and Crosson (45) proposed that ParD interactions with ParE do not induce large conformational changes in the toxin. Because *C. crescentus* ParD and *V. cholerae* ParD2 are similar (50% identity), we suspect ParD2 and ParE2 interact in a similar manner as their *C. crescentus* homologues. If this is the case, it is tempting to propose that the inability of ParD2 to reverse ParE2 toxicity stems from the absence of significant changes in ParE2 structure when it is bound by ParD2. Thus, if ParE2 is bound to gyrase, ParD2 binding may not lead to release gyrase from ParE2. A challenge for future studies will be to define if and how ParD2 prevents ParE2 interaction with GyrA *in vivo*. Recently Hallez *et al.* (46) reported that PaaA, an antitoxin for a ParE homologue in *E. coli* O157, altered the toxin subcelluar localization. It is possible that ParD2, which lacks similarity to PaaA, blocks ParE2 toxicity in a similar fashion as PaaA by sequestering the toxin away from gyrase.

Although there is considerable controversy regarding the physiologic function of chromosomal TA loci, previous work has led to the suggestion that such loci contribute to genome integrity. For example, two *Vibrio vulnificus* superintegron-encoded TA loci (*relBE1* and *parDE1*) appear to prevent large scale chromosome loss (6). The *parDE2* locus and likely the two *parDE1* loci in the *V. cholerae* chromosome II superintegron may also function to promote the integrity of the *V. cholerae* genome, which like all members of the Vibrionaceae is divided between two chromosomes. *V. cholerae* strains that lose chromosome II undergo a characteristic series of cytologic changes culminating in cell death (47). One of the phenotypes observed after chromosome II loss is the guillotining of the remaining chromosome I. The DNA damage observed in the cells lacking chromosome II resembles the catastrophic effect of ParE2 on *V. cholerae* chromosomal DNA shown in Fig. 6. Thus, *parDE2* might contribute to *V. cholerae* genome integrity via a mechanism similar to post-segregational killing. After loss of chromosome II (and the *parDE2* locus), the more stable ParE2 would outlive the ParD2 antitoxin and poison DNA gyrase leading to the cleavage of chromosome I. We are currently exploring whether the *V. cholerae parDE* loci contribute to destruction of chromosome I when chromosome II is lost from cells.

A Novel Mechanism for Poisoning Gyrase—Our findings suggest that ParE2 interacts with gyrase at a site different from that of other agents that target this enzyme (Fig. 9). Even though we found that, like CcdB (51, 55), ParE2 binds to GyrA59 with high affinity (Fig. 5), ParE2 did not interact with GyrA14 (Fig. 5), unlike the CcdB family of toxins. Furthermore, ParE2 bound to GyrA saturated with CcdB (Fig. 5*F*). The locations of the residues conferring CcdB and Nal resistance are mapped on to the crystal structure of GyrA59 in Fig. 9. Because these residues are mostly found in the core of the GyrA subunit, it is likely that ParE2 interacts somewhere else on this gyrase subunit.

We found that ParE2, like CcdB and quinolones, can stabilize gyrase-DNA cleavage intermediates (Fig. 6). Covalent gyrase-DNA intermediates are formed during the gyrase catalytic cycle after the enzyme binds and cleaves the "G segment" of the DNA duplex (48). Ordinarily (in the absence of toxin), gyrase then transports the "T segment" through the resulting "gate" and then reseals the gap, thereby altering DNA topology. In contrast to quinolones and CcdB, ATP is required for ParE2 to stall the gyrase cleavage complex (Fig. 8). Although the precise role of ATP in the gyrase cycle is still not clear, it is generally accepted that its binding and hydrolysis trigger conformational changes in the entire enzyme complex (19). Upon binding ATP, the N-terminal ATPase domains of GyrB dimerize and close the "ATP-operated clamp," capturing the T segment, which is then passed through the transiently cleaved G-segment. It has been suggested that ATP hydrolysis provides the driving force for transport of the T segment, when it passes from the "top" to the "bottom" of the enzyme (49). The latter step is thought to be essential for the gyrase supercoiling cycle (19). Thus, it is possible that changes in gyrase structure that accompany DNA wrapping and ATP hydrolysis, such as T segment top-down passage and the opening of the DNA gate, are required for ParE2 to interact with gyrase and inhibit its supercoiling activity. Because similar conformational changes in gyrase structure likely do not occur during enzyme relaxation of DNA, which proceed in the absence of ATP and DNA wrapping (19, 50), ParE2 is incapable of inhibiting gyrase relaxation activity. We nevertheless detected ParE2 binding to gyrase on the chip in the absence of ATP. However, previous studies have shown that gyrase can adopt atypical conformations when bound to SPR chips (51). Additionally, it is possible that ParE2 gyrase interactions are ordinarily constrained by the presence of DNA in supercoiling and relaxation assays.

Overall, the action of ParE2 on gyrase resembles the action of CcdB. However, there clearly are differences; for example, the requirement of ATP for ParE2 toxic action. It is likely that the two toxins do not share the same binding site, as the GyrA14 peptide did not abrogate the toxic action of ParE2. Given the extensive nature of the GyrA-GyrA interface that is likely to be transiently revealed during the ATP-dependent supercoiling process, we suggest that ParE2 may bind somewhere in this interface region. This is a topic for future investigation.

Acknowledgments—We thank Dr. Brigid Davis and Monica P. Hui for helpful discussions and comments on manuscript.

REFERENCES

1. Jensen, R. B., and Gerdes, K. (1995) *Mol. Microbiol.* **17,** 205–210
2. Ogura, T., and Hiraga, S. (1983) *Cell* **32,** 351–360
3. Buts, L., Lah, J., Dao-Thi, M. H., Wyns, L., and Loris, R. (2005) *Trends Biochem. Sci.* **30,** 672–679
4. Pandey, D. P., and Gerdes, K. (2005) *Nucleic Acids Res.* **33,** 966–976
5. Ramage, H. R., Connolly, L. E., and Cox, J. S. (2009) *PLoS Genet* **5,** e1000767
6. Szekeres, S., Dauti, M., Wilde, C., Mazel, D., and Rowe-Magnus, D. A. (2007) *Mol. Microbiol.* **63,** 1588–1605
7. Engelberg-Kulka, H., Amitai, S., Kolodkin-Gal, I., and Hazan, R. (2006) *PLoS Genet.* **2,** e135
8. Tsilibaris, V., Maenhaut-Michel, G., Mine, N., and Van Melderen, L. (2007) *J. Bacteriol.* **189,** 6101–6108
9. Van Melderen, L., and Saavedra De Bast, M. (2009) *PLoS Genet* **5,** e1000437
10. Maxwell, A. (1997) *Trends Microbiol.* **5,** 102–109
11. Roberts, R. C., Ström, A. R., and Helinski, D. R. (1994) *J. Mol. Biol.* **237,** 35–51
12. Easter, C. L., Sobecky, P. A., and Helinski, D. R. (1997) *J. Bacteriol.* **179,** 6472–6479
13. Jiang, Y., Pogliano, J., Helinski, D. R., and Konieczny, I. (2002) *Mol. Microbiol.* **44,** 971–979
14. De Jonge, N., Buts, L., Vangelooven, J., Mine, N., Van Melderen, L., Wyns, L., and Loris, R. (2007) *Acta Crystallogr. Sect. F Struct. Biol. Cryst. Commun.* **63,** 356–360
15. Schoeffler, A. J., and Berger, J. M. (2008) *Q. Rev. Biophys.* **41,** 41–101
16. Reece, R. J., and Maxwell, A. (1991) *Crit. Rev. Biochem. Mol. Biol.* **26,** 335–375
17. Kampranis, S. C., and Maxwell, A. (1996) *Proc. Natl. Acad. Sci. U.S.A.* **93,** 14416–14421
18. Reece, R. J., and Maxwell, A. (1991) *Nucleic Acids Res.* **19,** 1399–1405
19. Nöllmann, M., Crisona, N. J., and Arimondo, P. B. (2007) *Biochimie* **89,** 490–499
20. Couturier, M., Bahassi el-M., and Van Melderen, L. (1998) *Trends Microbiol.* **6,** 269–275
21. Anantharaman, V., and Aravind, L. (2003) *Genome Biol.* **4,** R81
22. Thoden, J. B., Sellick, C. A., Timson, D. J., Reece, R. J., and Holden, H. M. (2005) *J. Biol. Chem.* **280,** 36905–36911
23. Dao-Thi, M. H., Van Melderen, L., De Genst, E., Buts, L., Ranquin, A., Wyns, L., and Loris, R. (2004) *Acta Crystallogr. D Biol. Crystallogr.* **60,** 1132–1134
24. Nieba, L., Nieba-Axmann, S. E., Persson, A., Hämäläinen, M., Edebratt, F., Hansson, A., Lidholm, J., Magnusson, K., Karlsson, A. F., and Plückthun, A. (1997) *Anal. Biochem.* **252,** 217–228
25. Smith, A. B., and Maxwell, A. (2006) *Nucleic Acids Res.* **34,** 4667–4676
26. Heidelberg, J. F., Eisen, J. A., Nelson, W. C., Clayton, R. A., Gwinn, M. L., Dodson, R. J., Haft, D. H., Hickey, E. K., Peterson, J. D., Umayam, L., Gill, S. R., Nelson, K. E., Read, T. D., Tettelin, H., Richardson, D., Ermolaeva, M. D., Vamathevan, J., Bass, S., Qin, H., Dragoi, I., Sellers, P., McDonald, L., Utterback, T., Fleishmann, R. D., Nierman, W. C., White, O., Salzberg, S. L., Smith, H. O., Colwell, R. R., Mekalanos, J. J., Venter, J. C., and Fraser, C. M. (2000) *Nature* **406,** 477–483
27. Bocs, S., Danchin, A., and Médigue, C. (2002) *BMC Bioinformatics* **3,** 5
28. Khlebnikov, A., Datsenko, K. A., Skaug, T., Wanner, B. L., and Keasling, J. D. (2001) *Microbiology* **147,** 3241–3247
29. Pedersen, K., Zavialov, A. V., Pavlov, M. Y., Elf, J., Gerdes, K., and Ehrenberg, M. (2003) *Cell* **112,** 131–140
30. Kamada, K., Hanaoka, F., and Burley, S. K. (2003) *Mol. Cell* **11,** 875–884
31. De Jonge, N., Garcia-Pino, A., Buts, L., Haesaerts, S., Charlier, D., Zangger, K., Wyns, L., De Greve, H., and Loris, R. (2009) *Mol. Cell* **35,** 154–163
32. Schumacher, M. A., Piro, K. M., Xu, W., Hansen, S., Lewis, K., and Brennan, R. G. (2009) *Science* **323,** 396–401
33. Brown, B. L., Grigoriu, S., Kim, Y., Arruda, J. M., Davenport, A., Wood, T. K., Peti, W., and Page, R. (2009) *PLoS Pathog.* **5,** e1000706
34. Bernard, P., and Couturier, M. (1992) *J. Mol. Biol.* **226,** 735–745
35. Kampranis, S. C., Bates, A. D., and Maxwell, A. (1999) *Proc. Natl. Acad. Sci. U.S.A.* **96,** 8414–8419
36. Loris, R., Dao-Thi, M. H., Bahassi, E. M., Van Melderen, L., Poortmans, F., Liddington, R., Couturier, M., and Wyns, L. (1999) *J. Mol. Biol.* **285,** 1667–1677
37. Dao-Thi, M. H., Van Melderen, L., De Genst, E., Afif, H., Buts, L., Wyns, L., and Loris, R. (2005) *J. Mol. Biol.* **348,** 1091–1102
38. Gellert, M., Mizuuchi, K., O'Dea, M. H., Itoh, T., and Tomizawa, J. I. (1977) *Proc. Natl. Acad. Sci. U.S.A.* **74,** 4772–4776
39. Sugino, A., Peebles, C. L., Kreuzer, K. N., and Cozzarelli, N. R. (1977) *Proc. Natl. Acad. Sci. U.S.A.* **74,** 4767–4771
40. Bernard, P., Kézdy, K. E., Van Melderen, L., Steyaert, J., Wyns, L., Pato, M. L., Higgins, P. N., and Couturier, M. (1993) *J. Mol. Biol.* **234,** 534–541
41. De Jonge, N., Hohlweg, W., Garcia-Pino, A., Respondek, M., Buts, L., Haesaerts, S., Lah, J., Zangger, K., and Loris, R. (2010) *J. Biol. Chem.* **285,** 5606–5613
42. Madl, T., Van Melderen, L., Mine, N., Respondek, M., Oberer, M., Keller, W., Khatai, L., and Zangger, K. (2006) *J. Mol. Biol.* **364,** 170–185
43. Oberer, M., Zangger, K., Gruber, K., and Keller, W. (2007) *Protein Sci.* **16,** 1676–1688
44. Garcia-Pino, A., Christensen-Dalsgaard, M., Wyns, L., Yarmolinsky, M., Magnuson, R. D., Gerdes, K., and Loris, R. (2008) *J. Biol. Chem.* **283,** 30821–30827
45. Dalton, K. M., and Crosson, S. (2010) *Biochemistry* **49,** 2205–2215
46. Hallez, R., Geeraerts, D., Sterckx, Y., Mine, N., Loris, R., and Van Melderen, L. (2010) *Mol. Microbiol.* **76,** 719–732
47. Yamaichi, Y., Fogel, M. A., and Waldor, M. K. (2007) *Proc. Natl. Acad. Sci. U.S.A.* **104,** 630–635
48. Horowitz, D. S., and Wang, J. C. (1987) *J. Biol. Chem.* **262,** 5339–5344
49. Baird, C. L., Harkins, T. T., Morris, S. K., and Lindsley, J. E. (1999) *Proc. Natl. Acad. Sci. U.S.A.* **96,** 13685–13690
50. Nöllmann, M., Stone, M. D., Bryant, Z., Gore, J., Crisona, N. J., Hong, S. C., Mitelheiser, S., Maxwell, A., Bustamante, C., and Cozzarelli, N. R. (2007) *Nat. Struct. Mol. Biol.* **14,** 264–271
51. Kampranis, S. C., Howells, A. J., and Maxwell, A. (1999) *J. Mol. Biol.* **293,** 733–744
52. Morais Cabral, J. H., Jackson, A. P., Smith, C. V., Shikotra, N., Maxwell, A., and Liddington, R. C. (1997) *Nature* **388,** 903–906
53. Guzman, L. M., Belin, D., Carson, M. J., and Beckwith, J. (1995) *J. Bacteriol.* **177,** 4121–4130
54. Lessl, M., Balzer, D., Lurz, R., Waters, V. L., Guiney, D. G., and Lanka, E. (1992) *J. Bacteriol.* **174,** 2493–2500
55. Simic, M., De Jonge, N., Loris, R., Vesnaver, G., and Lah, J. (2009) *J. Biol. Chem.* **284,** 20002–20010